THE ASTROPHYSICAL JOURNAL, 445:231–239, 1995 May 20

A COLD MASSIVE INTERSTELLAR CLOUD WITHIN 120 PARSECS OF THE SUN: K I OPTICAL AND H I RADIO OBSERVATIONS

JOAQUÍN TRAPERO,[1] JOHN E. BECKMAN, AND MIQUEL SERRA-RICART
Instituto de Astrofísica de Canarias, 38200-La Laguna, Spain;
trapero@yerkes.uchicago.edu, jeb@iac.es, mserra@iac.es

RODNEY D. DAVIES AND ROBERT A. WATSON[2]
Nuffield Radio Astronomy Laboratories, Jodrell Bank, Macclesfield, Cheshire SK11 9DL, UK;
rdd@jb.man.ac.uk, raw@iac.es

AND

RAMÓN J. GARCÍA LÓPEZ[3]
Department of Astronomy, The University of Texas at Austin, RLM 15.308, Austin TX 78712-1083; rgl@iac.es
Received 1994 May 9; accepted 1994 December 1

ABSTRACT

We first discovered the presence of a particularly massive cloud in the neighborhood of the Sun, close to the Galactic plane in the direction of Perseus, toward $l = 150°$, $b = -10°$, using interstellar absorption by the 7699 Å resonance line of K I (Trapero et al. 1992). In the present investigation we show the results of mapping the cloud in the 21 cm line of H I, supplemented by further K I observations. This combination is particularly effective, since the K I observations give us distances, within close limits, and accurate velocities of the single strong interstellar component detected along each line of sight, which enables us to identify the cloud as seen in absorption in the H I spectra, from among many emission components due to more distant clouds in the plane. The absorption spectra in H I at 21 cm can then be used to find temperatures and to carry out more comprehensive mapping than using K I. We find that the cloud has kinetic temperatures going down to 30 K, densities in the range up to 70 cm^{-3}, a diameter of ~ 15 pc, and a mass of some 1300 $M_\odot$. The cloud is a good candidate to contain a molecular core.

Subject headings: ISM: abundances — ISM: atoms — ISM: clouds — radio lines: ISM

1. INTRODUCTION

Exploration and mapping of the gas in the local spiral arm of the Galaxy, within 200 pc of the Sun, is one of the best ways to derive and understand the structure throughout the interstellar medium (ISM). The questions addressed are as follows: what fraction of the medium is in each of the phases, namely the hot, warm, cool, and molecular phases which are known to be stable and distinct; what are the physical conditions, such as temperature, density, and degree of ionization in each phase; what are the sources of energy input; and what dynamical effects are taking place? The reasons that the local interstellar medium (LISM) is so useful here are analogous to those which made the Sun a touchstone for many aspects of stellar physics. Optical and UV studies of the general ISM have most commonly been performed via absorption spectroscopy against background stars; in the best resolved spectra, with highest S/N ratios, one finds, basically, a blend of multiple components due to many individual IS clouds along any line of sight. Measurements of this kind in the LISM, however, yield very few components, often only one (or even zero), which makes accurate derivation of the properties of each individual cloud much easier. Observing the LISM in absorption implies using nearby stars as background illumination, yielding spectra of high intensity, from which accurate equivalent widths and radial velocities for the IS clouds are obtainable. The short lines of sight involved imply relatively good linear resolution on an IS cloud, even though the OB star sources may be sparsely arrayed in angle. Finally, and most significantly, local stars have well-measured distances which allow us good estimates of LISM cloud distances, and hence sizes, masses, and other parameters of interest.

The present article is part of a long-term systematic study of the LISM using UV, visible, and, now, radio spectroscopy. Starting with the Mg II *h* and *k* resonance doublet, measured with *IUE*, which probes the "warm" phase of the LISM in the range $5 \times 10^3 \lesssim T_K \lesssim 10^4$ K (Vladilo et al. 1985; Molaro, Vladilo, & Beckman 1986; Génova et al. 1990), we went on to observe the K I line at 7699 Å (also a member of a resonance doublet), which is an excellent probe of the cool phase, at $T_K \lesssim 100$ K. In Trapero et al. (1992) we showed how this K I line explores the range of H I column densities between some 10^{20} cm^{-2} and a few times 10^{21} cm^{-2}, where cool clouds are found.

The method for measuring the physical parameters of a cloud is simple, but effective, and warrants a brief description here. After finding a strong narrow IS K I absorption line—with an equivalent width of few tens of mÅ—in the spectrum of an O or B star within 200 pc of the Sun, one observes lines of sight to stars adjacent in angle, and within the same distance range; some spectra have strong IS absorptions, while others show a little or none. The radial velocity values can be used to determine whether the absorptions are due to one or more clouds; multiple components, or jumps in radial velocity of 3,

[1] Present address: University of Chicago, Yerkes Observatory, Williams Bay, WI 53191-0258.
[2] Present address: Instituto de Astrofísica de Canarias, 38200-La Laguna, Spain.
[3] Also Instituto de Astrofísica de Canarias, 38200-La Laguna, Spain.

or more, km s^{-1}, are due to clouds other than the original cloud entering the line of sight. The use of a set of closely grouped lines of sight may allow us to establish the size of the cloud. The outline is marked by stars with no absorption at the required velocity. A lower limit on the distance is deducible from stars nearer than the cloud, and close to its center in angle, which show no absorption at the measured velocity while upper distance limits come from the closest stars in which appropriate K I absorptions are seen at full strength.

Given the distance, the angular size can be converted into a linear size, and assuming spherical symmetry the diameter perpendicular to the line of sight can be set equal to the column length along the line of sight. Some evidence for, at least approximate, spherical symmetry comes from the observation (Trapero et al. 1992) that the range of sizes of cool LISM clouds in a given direction in the Galactic plane is comparable to the range of sizes of these clouds toward galactic longitudes in a perpendicular direction. From the measured column length, and an H I column density derived from the K I line equivalent width (Trapero et al. 1992) we can infer a mean number density for H I through the cloud: typical values of tens per cubic centimeter are in fact found for this cloud population. We can go further, albeit with some degree of speculation and uncertainty, and infer a mean cloud temperature assuming a canonical value for the IS pressure close to the Galactic plane (Jura 1975; Jenkins, Jura, & Loewenstein 1983) and pressure equilibrium rather than gravitational equilibrium. Typical cool cloud values found in this way are in the range $T < 100$ K, assuming a value for p/k of 3600 K cm^{-3}. Multiplying the cloud volume by the derived density yields the cloud mass: here one finds typical masses of a few tens to a couple of hundred solar masses, less than the Jeans mass corresponding to these typical conditions, which is a post hoc justification for making the assumption of pressure equilibrium. The error limits entailed by this procedure allow us to estimate the mass of an individual cloud to within a factor 2. One can then go on to use a survey of such objects (Trapero et al. 1992) to show that although they occupy only some 5% of the local volume, they make up a substantial fraction of the LISM mass, perhaps as much as 90% of it.

In the course of our first look at the cold component of the LISM using K I we encountered one cloud, for which we had but two lines of sight, which showed greater column densities and a significantly greater initial estimate of the mass than any other single cloud. It lies in the direction $\alpha = 3^h30^m$, $\delta = 44°50'$, corresponding to $l = 150°$, $b = -10°$, toward Perseus, and can be made out as a region of somewhat reduced intensity on the Palomar Observatory Sky Survey plates, and at a distance of less than 140 pc from the Sun, as inferred from the distances to the two stars HD 23552 and HD 21455, in whose spectra the strong K I detections were made. Although near, the hydrogen column density, estimated as some 2×10^{21} cm^{-2}, is high. This appeared to be quite a massive cloud, with an initial rough estimate of 1000 $M_\odot$ for its mass. We felt that the presence of such a massive IS cloud in the solar neighborhood warranted a more concentrated observational campaign, of which the results are presented in the present paper. We describe the observations in K I and H I, the data analysis, and our new estimates of the extent, and the mass of the cloud, including the result of a neural network approach to the relatively sparse data set at 21 cm. Finally we speculate on the possibility of finding a molecular cloud at the center of this cold, massive object.

2. OBSERVATIONS

2.1. *The* K I *Line*

Our new observations in the 7699 Å resonance line of K I were obtained using the IACUB (McKeith et al. 1993) spectrograph at the Cassegrain focus of the 2.5 m NOT telescope, La Palma, Canary Islands, Spain, during 1992 December. The instrument, combined with a CCD camera, yielded a slit-limited spectral resolution $\lambda/\Delta\lambda$ of 5×10^4 when used, as in the present study, to optimize the spectrograph-telescope match (this resolution corresponds to an image of 0".5 on the sky). Exposures were obtained in periods of 30 minutes at a time, to limit the spurious signals of cosmic rays in the CCD. A characteristic total exposure for a 6th mag star was 1 hr giving a S/N of some 100. Spectra were flat-fielded, sky-subtracted, cosmic-ray–corrected, and wavelength-calibrated using standard programs in the IRAF[4] (Image Reduction and Analysis Facility) software package (Tody 1986). Figure 1 shows two sample spectra. Accurate wavelength calibration in this range is facilitated by the presence of a series of telluric O_2 doublets, which are always present, invariant in velocity, and unresolved. For K I lines of more than 10 mÅ equivalent width in spectra with S/N ~ 100, velocity calibration can be achieved with an error of no more than 1 km s^{-1}. This precision is very important for identifying and setting limits to individual clouds in K I, and it proved equally important for our subsequent analysis of H I. The equivalent widths were obtained using the Bandfit computer program, written by G. Vladilo and modified by R. García López, which fits one or more Gaussians to an observed spectral line and measures their individual wavelengths, full widths to half-maximum, and equivalent widths. The precision of each fit depends, of course, on the S/N ratio of the spectrum measured and the strength of the line observed; with typical practical values for S/N ratio here, we could set

[4] IRAF is distributed by the National Optical Astronomy Observatories, which is operated by the Association of Universities for Research in Astronomy, Inc. (AURA) under cooperative agreement with the National Science Foundation.

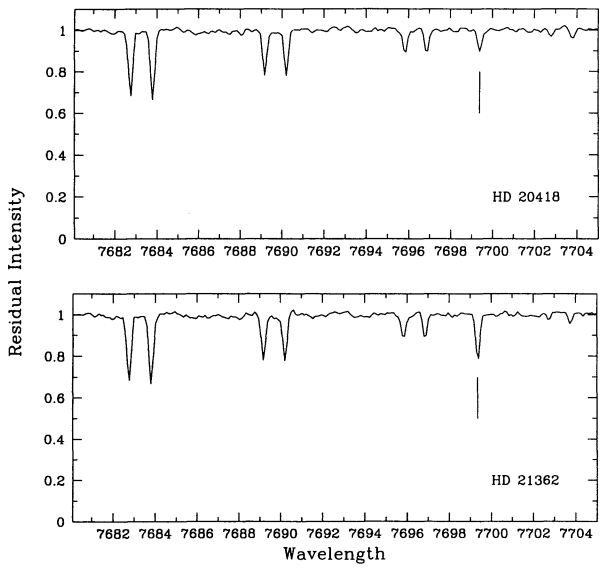

FIG. 1.—Examples of the optical data used: spectra of the stars HD 20418 (*above*) and HD 21362 (*below*) in the range of the interstellar K I line at 7699 Å (marked with a line).

TABLE 1

STARS OBSERVED

Identifier	Star (HD)	l	b	d (pc)	Spectral Type	m_v	$v \sin i$ (km s^{-1})
a	20418	145°.74	−6°.12	130	B5 V	5.03	298
b	23383	145.85	+1.10	136	B9 V	6.10	415
c	21362	147.19	−5.46	153	B6 V	5.58	355
d	20315	148.85	−11.36	121	B8 V	5.47	269
e	21551	148.42	−6.83	137	B8 V	5.82	334
f	21803	150.61	−9.18	483	B2 IV	6.41	...
g	24504	151.94	−4.33	137	B6 V	5.37	286
h	23300	152.00	−7.11	166	B6 V	5.66	...
i[a]	23552	149.16	−2.90	137	B8 V	6.14	250
j[a]	21455	148.93	−7.80	150	B7 V	6.24	150

[a] Observed in 1988 October. Already discussed in Trapero et al. 1992.

lower limits of 2 mÅ to the equivalent width and ± 1 km s^{-1} to the velocity of a detected feature. In Table 1 we list the stars observed toward the Perseus cloud, and in Table 2, their respective observed parameters. The two stars already discussed in Trapero et al. (1992) are indicated; the other stars are newly observed for K I. We can see that equivalent widths of 25 mÅ or more, equivalent to $N(\text{H I}) > 1.3 \times 10^{21}$ cm^{-2} are found in four of the new positions. We can also see that three stars show considerably weaker absorptions, while one shows an unmeasurable absorption within the observational limit of 2.5 mÅ. Combining all the information along the lines of sight represented in Table 2 we can obtain new, more useful, estimates for the mass and extent of the cloud, but these are still quite limited, and at this stage we found it valuable to explore the direction of the cloud in the 21 cm line.

2.2. *The 21 Centimeter Line*

The H-line observations were carried out during 1992 November with the 76 m Lovell Telescope of the Nuffield Radio Astronomy Laboratories, Jodrell Bank, which has a FWHM beamwidth of 12′. The dual-polarization receiver had a system noise of 45 K and provided two spectra each with a bandwidth of 2.5 MHz giving 512 channels with a separation of 4.88 kHz (1.03 km s^{-1}). The rms noise temperature per channel in each 10 minute spectrum was 0.05 K.

The brightness temperature calibration was made using the standard region S7 (Williams 1973). The observed spectra were reduced using the interactive Spectral Line Analysis Package (SLAP) developed at Jodrell Bank by Staveley-Smith (1985) which includes the standard gain-elevation correction for the

TABLE 2

INTERSTELLAR K I LINES OBSERVED

Identifier	Star (HD)	$W_{\text{K I}}$ (mÅ)	N(K I) ($\times 10^{11}$ cm^{-2})	N(H I) ($\times 10^{20}$ cm^{-2})	V_{LSR} (km s^{-1})
a	20418	26.0	1.9	14.0	+4.4
b	23383	<2.5	<0.2	<2	...
c	21362	52.3	4.3	16.0	+3.4
d	20315	12.5	0.9	9.7	+4.8
e	21551	13.5	1.0	11.0	+2.5
		2.7	0.2	2	+8.2
f	21803	70.8	6.3	18.0	+1.0
g	24504	26.0	1.9	14.0	+2.4
h	23300	11.8	0.8	9.2	+1.0
i	23552	105.6	10	20.0	+0.7
j	21455	105.3	10	20.0	+1.8
		16.3	0.95	10.1	+7.4

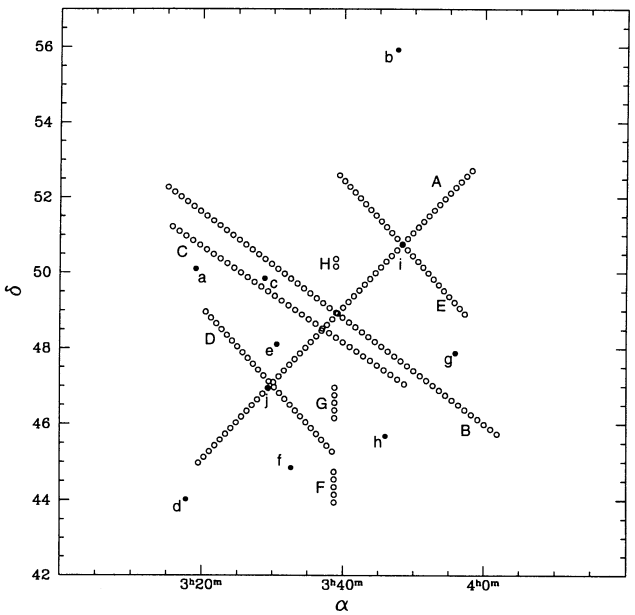

FIG. 2.—Sky directions observed in H I at 21 cm (*open circles*). The individual scans are labeled A to H. Filled circles indicate the directions to stars observed in K I and are lettered a through j following Table 1.

Lovell Telescope. The effects of spillover in the sidelobes of the telescope (Kalberla, Mebold, & Reif 1982) were removed using the program SPILLSUB (see, for example, Willacy 1990) in combination with the Bell Telephone Laboratories All-Sky H I Survey (Stark et al. 1992).

We used the K I data to define the approximate dimensions of the cloud and then observed points on lines through the cloud, extending them beyond the region defined optically. Figure 2 shows the positions for which H-line spectra were taken; beam centers were separated by 0°.2 along each scan.

Figure 3 presents an H I spectrum from a position ($\alpha = 3^{\text{h}}28^{\text{m}}54^{\text{s}}$, $\delta = 47°23'20''$) near the center of the cloud. It

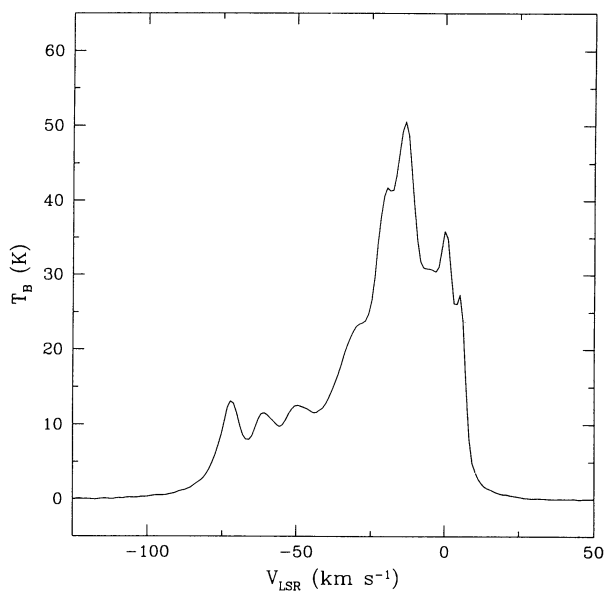

FIG. 3.—Sample spectrum at 21 cm toward a sky point on scan A. The Perseus cloud signature is the small sharp absorption at +3 km s^{-1}.

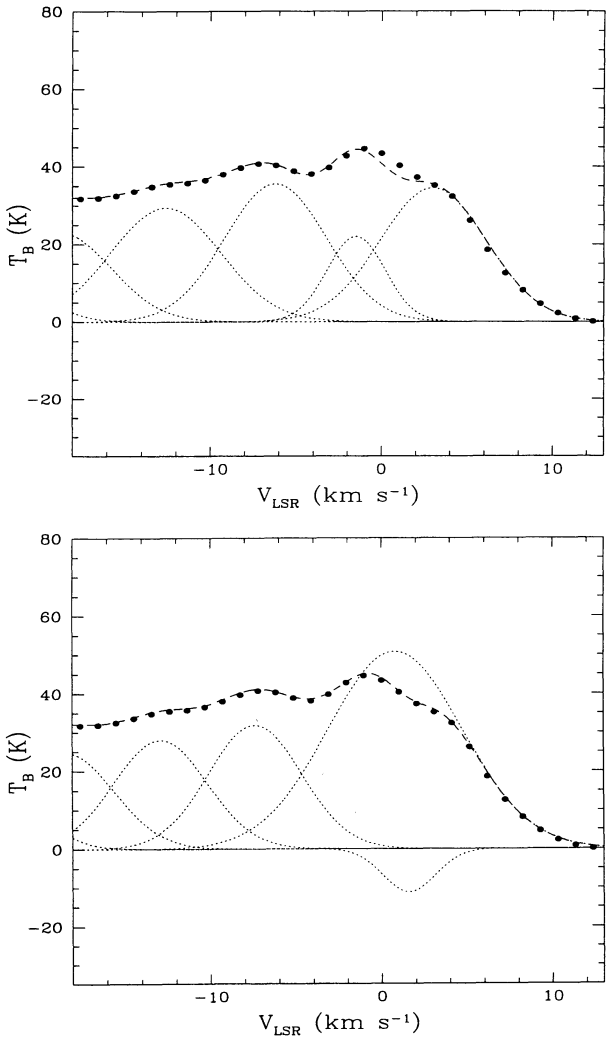

FIG. 4.—Comparison of two attempts to fit a portion, between $V_{LSR} = -18$ km s^{-1} and $V_{LSR} = +13$ km s^{-1}, of one of the H I spectra from scan C, using emission profiles only (*upper panel*) and a single absorption against the pseudo-continuum produced by emissions from the background clouds (*lower panel*). The fit using the absorption (at a radial LSR velocity coincident with the value obtained from the K I absorptions) is clearly better. *Dotted Gaussians*: individual components of the fit. *Dashed curve*: sum of the Gaussians. *Filled circles*: observed spectra.

clearly contains H I emission from many clouds along this line of sight extending out to the Perseus arm ($v = -60$ to -40 km s^{-1}) some 3 kpc distant.

On searching for the H I associated with the K I absorption at $+2$ km s^{-1}, it was evident that the H I was in absorption rather than emission. Such absorption is known in nearby dense clouds such as the large H I cloud (Riegel & Crutcher 1972; Crutcher & Riegel 1974) in the direction of the Galactic center; the absorption line widths are narrower than those seen in emission. In our own data we can reproduce the observed spectra by model-fitting with Gaussians which include an absorption feature at a LSR radial velocity of $+2$ km s^{-1} rather than an adjacent emission feature. In Figure 4 we show a pair of comparison fits in which the trial spectrum using only emission components is clearly inferior to the fit using an absorption component at the velocity predicted from the K I measurements.

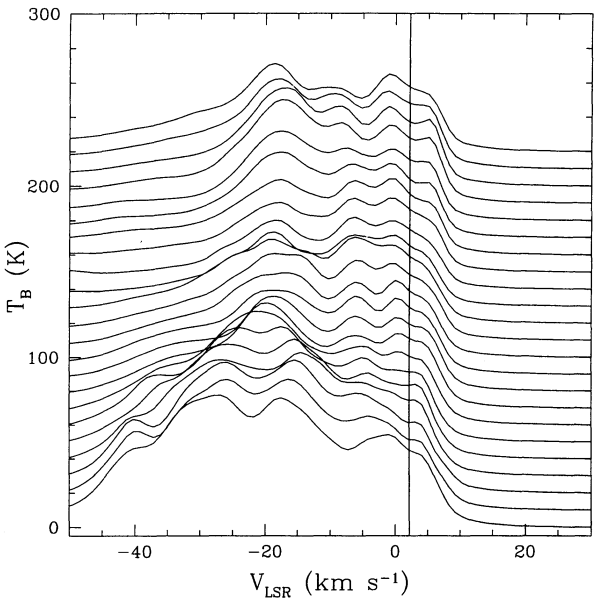

FIG. 5.—Set of spectra taken along a single scan (scan A), in the range of V_{LSR} from -50 km s^{-1} to $+30$ km s^{-1}. The lowest spectrum is not shifted with respect to the T_b axis, while the others are successively plotted at intervals of 10 K, for clarity. The vertical line at $V_{LSR} = +2$ km s^{-1} shows the velocity of the absorption feature predicted for the cloud under observation, from the K I absorptions.

In Figure 5 we present a set of spectra taken along scan direction A specified in Figure 2. It is noteworthy that the absorption component at $+2$ km s^{-1} shows the same velocity across the whole cloud, indicating that there is no significant rotational velocity. The absorption Gaussian is always narrower than that of the emission components from the background clouds as would be expected for a cooler object. These properties—the velocity invariance and narrow line width—give us the confidence that we are dealing with a genuine set of absorption features, in spite of the relatively low contrast due to the fact that the temperature difference between the cloud and the background is not especially large.

3. DELIMITING THE CLOUD WITH K I OBSERVATIONS

In Table 2 we show the results obtained from each of the lines of sight observed in K I. The total column density of hydrogen $N(\text{H I} + \text{H}_2)$ is deduced from the $N(\text{K I})$ value in two steps. We can estimate the density in sodium, $N(\text{Na I})$ from the relation $N(\text{Na I}) = 60 \times N(\text{K I})$ obtained empirically by Hobbs (1976) and confirmed by Chaffee & White (1982). The uncertainty here, due to variations in the ratio as temperatures vary, can be estimated at $\pm 20\%$ in the range of column densities sampled. Using the empirical relation $\log N(\text{H I} + \text{H}_2) = \log [N(\text{Na I}) + 9.09]/1.04$ from Ferlet, Vidal-Madjar, & Gry (1985), we obtain an estimate of the total column density in hydrogen. This relation gives reliable values below $N(\text{H I} + \text{H}_2) = 10^{21}$ cm^{-2}, but above this value we must estimate $N(\text{H I} + \text{H}_2)$ from an empirical fit to the data points of Ferlet et al. (1985), in their Figure 1. The total H I + H_2 column densities are reliable to $\pm 40\%$, and the LSR radial velocities to within ± 1 km s^{-1}.

It is possible to try to calculate the total hydrogen column density toward a certain star directly from its color index. We

have performed this procedure in order to compare with the values obtained using the K I measurements, and although we obtain good consistency toward HD 21803, HD 23552, and HD 21455, in general the value calculated from the color index is between a factor 2 or 3 lower. The fact that the three stars with the highest absorptions in K I are the ones which show the best agreement, shows the difficulty in the accurate use of reddening $E(B-V)$ lower than 0.3 and, on the other hand, the reliability of the use of the K I absorptions for high column densities.

We detected absorption features produced by the cloud in all but one of the stars. In Figure 6 we have plotted the distribution of the stars on the sky, with their corresponding hydrogen column densities. We have also shown the position of 48 Per, in which Hobbs (1969) detected no measurable interstellar absorption at the radial velocity which corresponds to the cloud. The two nondetections in Figure 6 seen as indicators of the angular cloud limits in the plane of the sky, in two directions, but the need to map more comprehensively to delimit the whole cloud is evident. The large circle in Figure 6 represents a first guess at the cloud area using K I data alone and assuming circular symmetry.

We can estimate an upper limit to the distance to the cloud as 120 pc from the detection in the line of sight toward HD 20315, the nearest of the group observed, whose distances are given in Table 1. We can also place a lower limit to the cloud distance from the observation that in the spectrum of δ Per (Hobbs 1974) at 82 pc from the Sun in the direction of the cloud center, there is no IS feature at the cloud velocity. We must point out that in the distances calculated for the different stars we have corrected the spectroscopic parallaxes using the tabulated colors of each star. If instead of using the extinction derived from the observed colors we calculate it from our own estimated column densities in hydrogen, via the ratio between $N(\mathrm{H\ I} + \mathrm{H_2})$ and the reddening $E(B-V)$ given in Bohlin, Savage, & Drake (1978), we obtain lower distances for all of the stars. Using these distances our cloud would be situated at somewhat less than 100 pc from the Sun (based on the distances to HD 20315 and HD 21455). It is not easy to resolve this discrepancy, but it is not disturbingly large, and for practical purposes we will take the more conservative approach of using the color-derived extinctions and distances, since they are based on fewer assumptions.

With this distance bracket, the diameter of the cloud, as represented by the large circle in Figure 6 is $\sim$14 pc, for a central distance of 105 pc, and assuming sphericity and a column density of 2×10^{21} cm^{-2} we find a mean density n_{H} of $\sim$70 cm^{-3} and a total mass of 1300 $M_{\odot}$. Then taking as a canonical value for the equilibrium pressure in the Galactic plane $p/k = 3600$ K cm^{-3} we find a characteristic average temperature along the line of sight of 50 K. These values differ somewhat from a previous estimate presented in Trapero et al. (1992), principally because of a slightly reduced estimate of the cloud diameter. Nevertheless the cloud is still found to be considerably more massive than the Jeans mass M_J at this temperature and pressure, which is $\sim$200 $M_{\odot}$, which implies probable magnetic support, and that the true cloud temperature should in fact be less than 50 K. To obtain a better look at the total mass, and possibly more direct measurement of the temperature, we will use the H I results given below.

A fair estimate of the mass M_B which can be supported by a magnetic field B inside a cloud of radius R is given (Mouschovias & Spitzer 1976) by

$$M_B = \frac{C_B \pi R^2 B}{G^{1/2}}, \qquad (1)$$

where G is the gravitational constant, and C_B is a constant which, for c.g.s. units, takes a value close to 0.1 (Tomisaka, Ikeuchi, & Nakamura, 1988), with B in gauss. For a cloud of radius 7 pc, equation (1) yields an estimate for M_B of $\approx 300 B_{-6}$, in units of $M_{\odot}$, where B_{-6} is now the field in μG. Thus for fields of order 3–4 μG characteristic of diffuse clouds, M_B would be of order 900–1200 $M_{\odot}$. If to this we add the Jeans mass, we can see that the cloud can in fact be stable against collapse, although it appears rather close to the limiting condition. Given all the uncertainties, both observational and theoretical, it is safest to say that there is no clear reason that this cloud has to be unstable against collapse. In fact, given its estimated density, it most probably contains higher local values of internal magnetic field than those cited above, which would tend to increase its stability.

The general direction of this cloud in the sky coincides with the α Per open cluster, and it is of interest to discuss any possible relation between the cloud and the cluster. Already in 1950 Roman & Morgan studying the cluster noticed a region of "moderately heavy absorption" and pointed out that the stellar colors measured indicate that the cluster may be behind this absorption. The distance to the cluster is estimated to be 160 pc (Prosser 1992) while most of our stars lie at less than 140 pc. But we have again to deal with the uncertainties of the distances calculated by spectoscopic parallax, the range in the distances calculated for stars which are members of the cluster is from 190 pc (α Per itself) to 130 pc. Prosser (1992) studied the membership of a great number of stars in the α Per cluster. According to that work, of the stars we consider here, HD

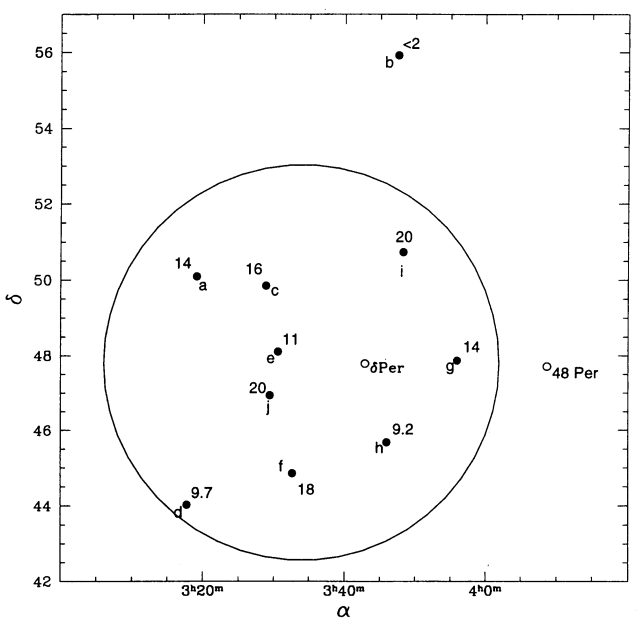

FIG. 6.—Distribution on the sky of the stars observed in K I, labeled a through j, as in Tables 1 and 2. The H I column density estimated from the K I absorption is indicated in units of 10^{20} cm^{-2}, at each position. We also include the position of 48 Per and δ Per (*small open circles*) where Hobbs (1969) and Hobbs (1974), respectively, found no measurable absorption at the velocity of the cloud. The large circle indicates a first estimate of the cloud angular diameter.

20418, HD 21362, HD 21551, and possibly HD 24504, are members of the cluster, while HD 20315 and HD 21455 are not and the rest are not included in his paper. The two stars identified as nonmembers have two of the highest column densities measured and HD 20315 is the nearest star of the stars observed, suggesting that the cloud is in fact situated some distance in front of the open cluster and may well not be directly physically connected to it.

4. MAPPING THE H I COLUMN DENSITY

Here we first describe how we obtained the two parameters: column density and temperature from the spectra observed, and then show how we inferred the shape and the mass of the cloud. As explained in § 2.2, each spectrum consists of a combination of emission lines from background clouds forming a heavily modulated continuum on which the narrower feature due to the cloud is superposed. The column density in H I can be inferred using a standard solution to the transfer equation (Verschuur 1974) in terms of the brightness temperature:

$$T_b(v) = T_s[1 - e^{-\tau(v)}] + T_c e^{-\tau(v)}, \quad (2)$$

where T_b is the observed brightness temperature in the line, T_s is the spin temperature of the cloud, and T_c is the temperature of the background source. This equation is capable of yielding the optical depth $\tau(v)$ in the cloud at the velocity v chosen, and we can then find the hydrogen column density by integrating across the line profile using

$$N_H = 1.823 \times 10^{18} \int_{-\infty}^{\infty} T_s \tau(v) dv . \quad (3)$$

However, in equation (2) we must deal with two unknowns: the optical depth $\tau(v)$, and the temperature T_s, and at this point our measurements can be called on to give useful circumstantial information. Using the upper limits to the temperature found along the lines of sight observed in K I, and the hydrogen column densities inferred, we can make an initial estimate for $\tau(v)$ in the 21 cm line and show that it ought to be greater than 2 or 3, i.e., that to a first approximation the assumption of optical thickness ought to be valid. Assuming this, we can obtain an approximate solution to equation (2) by letting T_b be equal to T_s, i.e., letting the spin temperature equal the observed brightness temperature in the line center. We can then compute a value for $\tau(v)$, and if we find that it conforms to our initial assumption of optical thickness we can go on to iterate for T_s. This procedure in practice showed good internal consistency and also continuity from point to point across the cloud.

For the value of the column density $N(\text{H I} + \text{H}_2)$ derived from our K I data in the direction of HD 23552 we obtain 2×10^{21} cm^{-2}, and from the spectrum in the 21 cm line in the same direction we obtain $N(\text{H I}) = 5.5 \times 10^{20}$ cm^{-2}. These two values are compatible and imply a column density $N(\text{H}_2)$ of molecular hydrogen of 7.3×10^{20} cm^{-2} in a ratio $N(\text{H I})/N(\text{H}_2)$ of 0.75. We can infer that it should be possible to detect this H_2 column density via the millimeter wave rotational spectrum of CO, in emission. Empirically the threshold for the formation of a significant molecular component has been found as $N(\text{H I} + \text{H}_2) \approx 5 \times 10^{20}$ cm^{-2} (Savage et al. 1977). In practice we would need to obtain the CO observations for this cloud in order to calibrate reliably the relation between $N(\text{K I})$ and $N(\text{H I} + \text{H}_2)$, obtained previously indirectly by an empirical $N(\text{H I} + \text{H}_2)$ versus $N(\text{Na I})$ calibration (Ferlet et al. 1985), with the Na/K abundance ratio. As stated above, the empirical relation cited appears to be linear up to around $N(\text{H I} + \text{H}_2) = 10^{21}$ cm^{-2}, and then breaks down, as higher column densities yield sufficient dust opacity to block the UV ionizing spectrum. This is just the range of physical interest in the present work, where we are dealing with the transition between conditions which favour the predominance of either atomic or molecular hydrogen. Combining K I measurements with those of H I and $\text{CO}(\text{H}_2)$ along a set of lines of sight through this cloud would help to quantify the proportion of atomic to molecular hydrogen as a function of the column density of dust shielding, as a complement to earlier UV spectroscopy (Savage et al. 1977).

Lada & Blitz (1988) suggested the division of diffuse clouds into two populations depending on the ratio of molecular to atomic gas. They termed those clouds with $N(\text{CO}) < 10^{14}$ cm^{-2} as "poor in CO" and those with $N(\text{CO}) > 10^{14}$ cm^{-2} as "rich in CO," finding a mean value for their sample of clouds in this latter population of $N(\text{CO}) = 4.2 \times 10^{16}$ cm^{-2}. If we go on to assume a CO-to-H_2 conversion factor which is essentially constant and take its value as $N(\text{CO})/N(\text{H}_2) = 5 \times 10^{-5}$ from Magnani, Blitz, & Wouterloot (1988), this mean value corresponds to a molecular hydrogen column density $N(\text{H}_2)$ of 8.4×10^{20} cm^{-2}. Thus we predict that the cloud discussed in the present paper may well turn out to be a member of this population "rich in CO," the same population in which Hobbs et al. (1988) classify the high-latitude MBM molecular clouds (Magnani, Blitz, & Mundy 1985).

We next turn to the determination of the cloud dimensions using all the data available. From our scans at 21 cm we could determine, using the method just described, the H I column density at each observed point on the sky; for each independent 12′ beam we started from the raw spectrum, extracted the absorption feature using the radial velocity as a tag, inferred the optical depth across the absorption profile, and integrated using equation (3). As is clear from Figure 2, the cloud was by no means uniformly sampled due to our need to optimize the strategy of detecting its main features in a limited observing period. We therefore adopted a technique which is well suited to the case, a technique which can interpolate sparse, or unevenly sampled data, that of the "neural network interpolator" (NNI) (see Serra-Ricart et al. 1994 for a detailed description of the method), which gave a stable solution, and the result is shown as an H I column density map in Figure 7*a*. The densest part of the cloud shows up very clearly, as do the edges, where these fall within the scope of the map. The "open" side of the diagram, toward higher R.A., clearly displayed in the isodensity contour map of Figure 7*b*, is that part of the cloud not mapped right to the edge.

Once we have the column density at each mapped point on the cloud, we can directly infer its total mass, by integrating over the whole zone, and in this way we obtain an H I mass of 660 $M_\odot$. To compare this estimate with the estimate of the total, atomic and molecular, mass of the cloud obtained in § 3, we can use the ratio $N(\text{H I})/N(\text{H}_2) = 0.75$, obtained above, which gives an upper limit for the total cloud mass of 2400 $M_\odot$. This is consistent with the value of 1300 $M_\odot$ obtained from the much less complete observations in K I, and confirms the fact that, in terms of the LISM, we are dealing with quite a massive cloud.

The cloud as delineated from the 21 cm measurements via the neural network interpolator does not conform entirely the shape outlined via the K I and other optical absorptions. For example toward the "open" side of the cloud Hobbs (1969)

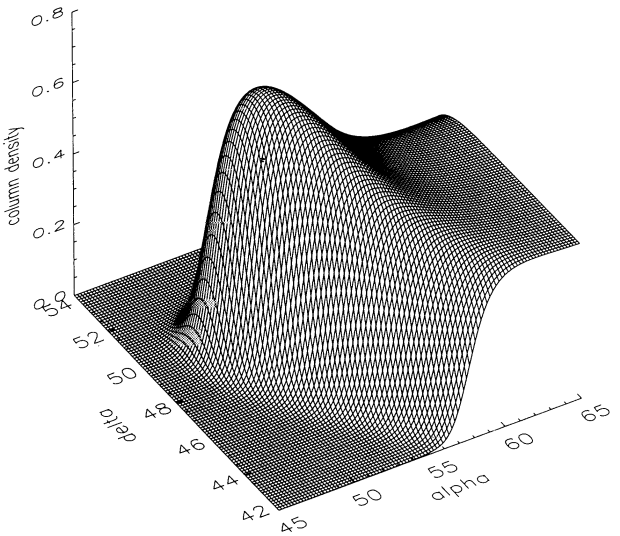

FIG. 7a

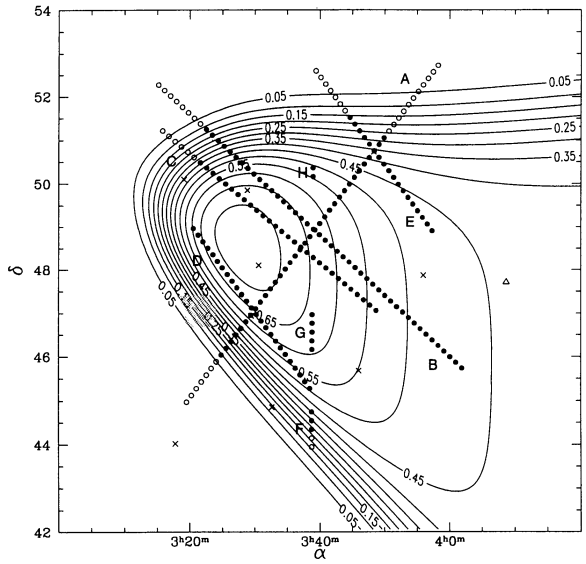

FIG. 7b

FIG. 7.—(*a*) Three-dimensional representation of the surface of column density in atomic hydrogen obtained by interpolation of the 21 cm data using the NNI (Serra-Ricart et al. 1994). The column density (vertical) axis is in units of 10^{21} cm^{-2}. (*b*) Contour map of equal column densities derived from (*a*), with the scan directions superposed. The contours are in units of 10^{21} cm^{-2}. Filled circles shows detections of the cloud at 21 cm, and open circles positions where no measurable absorption was detected. Stars observed in K I are indicated by crosses and 48 Per with a triangle. Note that the partial H I map leaves the cloud "open" to the east, but the optical nondetection at 48 Per allows us to set a limit to its extent in that direction.

found no measurable optical absorption at the appropriate velocity in the direction of 48 Per, which implies that there is, in fact, an edge to the cloud in this direction. Again, the star HD 20315 appears to be outside the cloud boundary, whereas our K I absorption shows that there is a hydrogen column density of 10^{21} cm^{-2} in that direction. Thus further observational work would be required to complete our measurements. Combining the estimated errors on the individual H I column densities, of some $\pm 15\%$, with these remaining geometrical uncertainties, we should place our best estimate of the cloud mass at $1500(\pm 450)\ M_\odot$. This uncertainty does not, of course affect the basic conclusion that the cloud is massive.

As mentioned above, the kinetic temperature of the cloud is calculated for each point observed in 21 cm by using equation (2). It was clear from the first values obtained that the temperature of the cloud is not constant along any of the scans obtained but shows smooth variation from point to point with upper and lower limits of ~ 45 K and ~ 30 K, respectively (see Fig. 8*a*).

We can assume that a cloud in the cold phase (McKee & Ostriker 1977) of the ISM ($T \lesssim 100$ K) such as the cloud treated in this paper, is surrounded by a warm ($T \lesssim 10^4$) layer and probably embedded in a pervasive hot ($T \sim 5 \times 10^5$ K) medium. If so it can be inferred quite straightforwardly that its center should be colder than its edges.

We applied the NNI in order to derive a temperature map of the cloud as a whole. The result obtained, shown in Figure 8*b*, confirms that the external region of the cloud shows higher temperatures, and the core exhibits a temperature minimum, as expected. Moreover the coldest part of the cloud coincides with the densest part. This cold ($T \sim 30$ K) and dense [N(H I) $\sim 7.5 \times 10^{20}$ cm^{-2}] core is the obvious place to look for CO emission.

5. CONCLUSIONS

In this paper we present observations, using the IACUB echelle spectrograph at the NOT telescope, of the K I line at 7699 Å toward eight stars lying in the direction of a massive dense cool cloud toward the constellation of Perseus, which we had previously detected, also in K I. We employ a technique developed in Trapero et al. (1992), identifying a single cloud by its radial velocity and comparing adjacent lines of sight to estimate the distance, size, density, mass, and temperature of the cloud. Using the new observations we find the cloud to lie between 80 pc and 120 pc of the Sun, with a diameter of ~ 14 pc, a density of 70 cm^{-3}, and a mass of 1300 $M_\odot$. The assumption of pressure equilibrium would set its kinetic temperature at 50 K, but as the cloud has a mass greater than the Jeans mass for its measured temperature and density, this value is almost certainly an upper limit.

We followed up our K I observations by measuring toward 200 sky points in the direction to the cloud, in the 21 cm line of H I using the 76 m Jodrell Bank radiotelescope. These observations gave us a much more complete map of the cloud and were complementary to the optical measurements, which could sample only a very limited number of lines of sight, those toward the appropriately situated O and B stars. As the cloud lies quite close to the Galactic plane, its signature appears as an absorption against the background of emission from numerous more distant clouds, confirming its rather low temperature.

The 21 cm observations covered ample zones of the cloud, but the observing strategy, aimed at finding the extent of the object with relatively limited observing time, led to a nonuniform sampling over its surface. We employed an interpolation technique using the neural network method (Serra-Ricart et al.

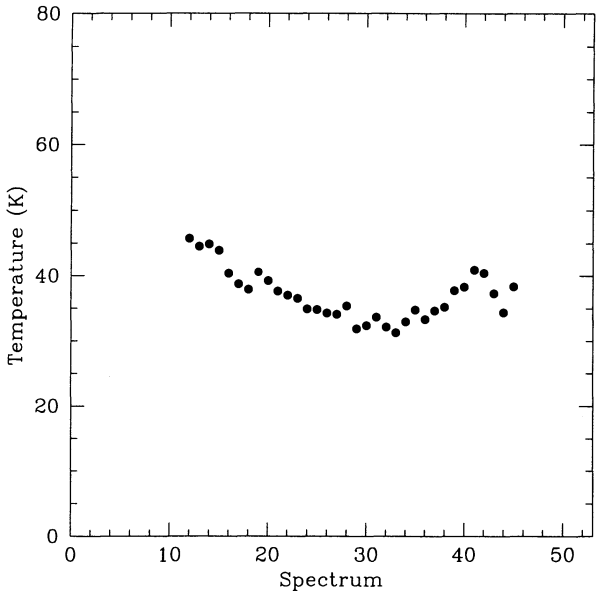

FIG. 8a

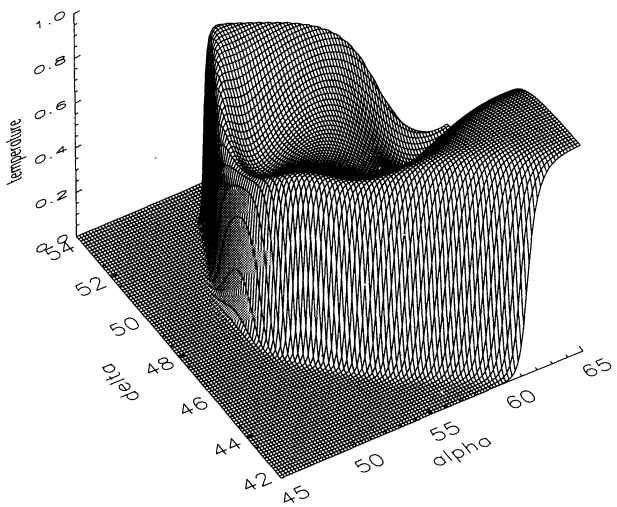

FIG. 8b

FIG. 8.—(*a*) Example of the variation of the kinetic temperature calculated in one of the scans (A) across the cloud. (*b*) Three-dimensional representations of the mean kinetic (spin) temperature of H I through the cloud, in the plane of the sky across Perseus cloud, as interpolated via the neural network (NNI) technique. The T_k axis is in units of 50 K. The cloud is seen to be systematically warmer at the edges than near the center. Note that the steep drop to zero outside the cloud indicates only that the temperature was set to zero there for computational purposes.

1994) in order to obtain maps of the cloud in column density of neutral hydrogen and in spin temperature. The mass estimate for the whole cloud, derived in this way from 21 cm data is 2400 $M_\odot$, which is well supported by the totally independent estimate of 1300 $M_\odot$ obtained from the K I data, especially noting that neither data set is complete. This mass is considerably larger than the Jeans mass corresponding to the density and temperature estimates of the cloud, and implies support from internal turbulence or magnetic pressure, or both.

The high mass, the presence of hydrogen column densities significantly greater than 10^{21} cm^{-2}, and the low measured internal temperature suggest the probable presence of a molecular component in the cloud. Comparison between our 21 cm and K I observations enable us to estimate a ratio H I/$H_2 \approx$ 0.75. It would be of interest to search directly for molecular emission using the millimetric rotational lines of CO.

We were able to infer an upper limit to the cloud temperature of 50 K, from the K I data, using the assumption of pressure equilibrium, but the 21 cm spectra enabled us to make more direct estimates of the kinetic temperature. These varied from some 30 K in the center of the cloud to some 45–50 K in the outer regions. The use of the neural network technique enabled us to make a fairly complete map of this temperature variation across the cloud, the coolest region coincides with the densest region in the center.

With the physical parameters estimated, this newly found Perseus cloud is one of the nearest ($d < 120$ pc) and coldest ($T < 30$ K) clouds in the solar neighborhood with substantial mass ($M \simeq 1300\ M_\odot$), and illustrative of the striking inhomogeneity of the local interstellar medium.

We are grateful to Jesús Rodríguez-Álamo for considerable help with the optical data reduction and to Jonathan V. Smoker for his assistance during the 21 cm observations at Jodrell Bank. We are happy to thank the referee, L. Blitz, and L. M. Hobbs for useful comments and advice. The Nordic Optical Telescope is operated on the island of La Palma by Lund Observatory in the Spanish Observatorio del Roque de Los Muchachos of the Instituto de Astrofísica de Canarias. The research on which this article is based was partially supported by grant PB 91-0525 of the DGICYT (Spanish Interministerial Commission for Science and Technology).

REFERENCES

Bohlin, R. C., Savage, B. D., & Drake, J. F. 1978, ApJ, 224, 132
Chaffee, F. H., & White, R. E. 1982, ApJS, 50, 169
Crutcher, R. M., & Riegel, K. W. 1974, ApJ, 188, 481
Ferlet, R., Vidal-Madjar, A., & Gry, C. 1985, ApJ, 298, 838
Génova, R., Molaro, P., Vladilo, G., & Beckman, J. E. 1990, ApJ, 355, 150
Hobbs, L. M. 1969, ApJ, 157, 135
———. 1974, ApJ, 191, 381
———. 1976, ApJ, 203, 143
Hobbs, L. M., Blitz, L., Penprase, B. E., Magnani, L., & Welty, D. E. 1988, ApJ, 327, 356
Jenkins, E. B., Jura, M., & Loewenstein, M. 1983, ApJ, 270, 88
Jura, M. 1975, ApJ, 197, 581
Kalberla, P. M. W., Mebold, U., & Reif, K. 1982, A&A, 106, 190
Lada, E. A., & Blitz, L. 1988, ApJ, 326, L69
Magnani, L., Blitz, L., & Mundy, L. 1985, ApJ, 295, 402
Magnani, L., Blitz, L., & Wouterloot, J. G. A. 1988, ApJ, 326, 909
McKee, C. F., & Ostriker, J. P. 1977, ApJ, 218, 148
McKeith, C. D., García-López, R. J., Rebolo, R., Barnett, E. W., Beckman, J. E., Martín, E. L., & Trapero, J. 1993, A&A, 273, 331
Molaro, P., Vladilo, G., & Beckman, J. E. 1986, A&A, 161, 339
Mouschovias, T. Ch., & Spitzer, L. 1976, ApJ, 210, 326
Prosser, C. F. 1992, AJ, 103, 488
Riegel, K. W., & Crutcher, R. M. 1972, A&A, 18, 55
Roman, N. G., & Morgan, W. W. 1950, ApJ, 111, 426

Savage, B. D., Bohlin, R. C., Drake, J. F., & Budich, W. 1977, ApJ, 216, 291
Serra-Ricart, M., Trapero, J., Beckman, J. E., Garrido, Ll., & Gaitan, V. 1994, AJ, in press
Stark, A. A., Gammie, C. F., Wilson, R. W., Bally, J., Linike, R. A., Heiles, C., & Hurwitz, M. 1992, A&AS, 79, 77
Staveley-Smith L. 1985, Ph.D. thesis, Univ. of Manchester
Tody, D. 1986, in Instrumentation in Astronomy. VI., ed. D. L. Crawford, Proc. SPIE, 627, 733
Tomisaka, K., Ikeuchi, S., & Nakamura, T. 1988, ApJ, 335, 239
Trapero, J., Beckman, J. E., Génova, R., & McKeith, C. D. 1992, ApJ, 394, 552
Verschuur, G. L. 1974, in Galactic and Extra-Galactic Radio Astronomy, ed. G. L. Verschuur & K. I. Kellermann (New York: Springer), 27
Vladilo, G., Beckman, J. E., Crivellari, L., Franco, M. L., & Molaro, P. 1985, A&A, 144, 81
Willacy, K. 1990, Ph.D. thesis, Univ. of Manchester
Williams, D. R. W. 1973, A&AS, 8, 505